

Modeling the interannual variability of Maipo and Rapel river plumes off central Chile

Julio Salcedo-Castro^{1,2,3}, Antonio Olita⁴, Freddy Saavedra⁵, Manuel Castillo⁶, Gonzalo S. Saldías^{7,8,9}, and Raúl Cruz-Gómez¹⁰

¹School of Earth and Atmospheric Sciences, Faculty of Science. Queensland University of Technology. Brisbane, Australia

²Sino-Australian Research Consortium for Coastal Management, School of Science, UNSW, Canberra, ACT, Australia

³Institute for Marine and Antarctic Studies, College of Sciences and Engineering, University of Tasmania, Hobart, Australia

⁴National Research Council - Institute of Atmospheric Sciences and Climate, Cagliari, Italy

⁵Laboratorio de Teledetección Ambiental (TeleAmb). Carrera de Geografía, Facultad de Ciencias Naturales y Exactas, Universidad de Playa Ancha, Chile

⁶Facultad de Ciencias del Mar y de Recursos Naturales, Universidad de Valparaíso, Chile

⁷Departamento de Física, Facultad de Ciencias, Universidad del Bío-Bío, Concepción, Chile

⁸Instituto Milenio en Socio-Ecología Costera (SECOS), Santiago, Chile

⁹Centro de Investigación Oceanográfica COPAS COASTAL, Universidad de Concepción, Chile

¹⁰Departamento de Física Universidad de Guadalajara. Blvd. Marcelino García Barragán y Calzada Olímpica C.P. 44840. Guadalajara, Jalisco, México

Correspondence: Julio Salcedo-Castro (julio.salcedocastro@qut.edu.au)

Abstract. River plumes have a direct influence on coastal environments, impacting coastal planktonic and benthic communities, including fishery resources. In general, the main drivers of river plume dynamics are the river discharge and the alongshore wind stress, whereas the tides and topography play a secondary role. In the Central part of Chile, rivers flowing into the eastern Pacific have a relatively short path on the land, with a high slope; further they are characterized by a mixed snow-rain regime.

5 This study aims to understand the interannual variability of the plumes of the Maipo and Rapel rivers in the Coastal/shelf area off Chile and its influence on local ocean dynamics. We used the Coastal and Regional Ocean Community model (CROCO), with 1 km resolution and 20 sigma levels, to simulate the ocean dynamics of the area over the period 2003-2011. The results show that the plume's area coverage and coastal ocean salinity are strongly correlated to the river discharges. The predominant southwestern wind controls the plumes orientation toward northwest; however, episodes of wind changing direction from
10 northwest in winter can reverse the plumes direction, making them squeezed to the coast and moving southward. Results also show, for the decade under evaluation, a salification trend linked to the severe droughts hitting Central Chile during the studied period. This salification determines a change in local dynamics.

Copyright statement. TEXT

1 Introduction

15 Among coastal ecosystems, river plumes are relevant marine areas because of their impact on physical and biogeochemical processes driving the seasonal and spatial dynamics of planktonic communities (D'sa and Miller, 2003; Mestres et al., 2003; Masotti et al., 2018). The most evident characteristics of river plumes are their low salinity, strong stratification, the generation of buoyancy-driven currents around the frontal area, and the higher turbidity associated with suspended solids. Although there are many forcings influencing the dispersion and dynamics of river plumes (e.g. tides, topography, inertia, local circulation, 20 Earth rotation and buoyancy) the river discharge and wind stress dominate the river plume dynamics (Fong and Rockwell Geyer, 2001; Lentz and Largier, 2006; Fernández-Nóvoa et al., 2015; Horner-Devine et al., 2015). For instance, Hetland (2010) demonstrated that the magnitude and length scale of cross-shore plume density changes are directly proportional to the river discharge. On the other hand, a recent work demonstrates that infra-gravity wave forcing has considerable influence on the plume dynamics in the near-field (Flores et al., 2022), which could influence mixing and cross-shore dispersion.

25 A proper description about the variability and trend of variables like salinity, nutrients and suspended solids in river plumes allows to estimate the condition of the catchment-coast system, where activities like deforestation, agriculture, and urban inputs can change the temporal pattern and influence of river discharges (Acker et al., 2009; Bainbridge et al., 2012; Martínez et al., 2018, 2022), in addition to the effects associated with climate change. For instance, by comparing different river systems, Acker et al. (2009) concluded that a decreasing trend in chlorophyll concentration within the river-influenced area is associated 30 with a reduction of the river discharges.

35 River plumes usually have high nutrient content and support primary production and algal biomass (Mallin et al., 2005; Peterson and Peterson, 2008; Kudela and Peterson, 2009). The influence of river plumes on larval transport and survival is related with their tolerance to osmotic shocks and their capacity to move vertically through the water column and density gradients (Bloodsworth et al., 2015). Different taxonomic groups will have different conditions to move and survive within river-influenced environments (Bloodsworth et al., 2015). Similarly, the influence of the river plume on sediments and benthos can be observed several (Forrest et al., 2007) to hundred (Grimes and Kingsford, 1996) kilometers from the river mouth. Other studies have demonstrated that the turbidity associated with the plume can influence the predation mortality of larval fish (Carreon-Martinez et al., 2014) and phytoplanktonic communities (Chakraborty and Lohrenz, 2015). The reduction of river discharges can have a negative impact on the fishery resources, biodiversity and ecological functions (Fan et al., 2022). 40 For instance, in central Chile, Vargas et al. (2006) described the influence of the Maipo river plume on the distribution of chlorophyll and barnacle larvae on the inner shelf.

45 Several studies have demonstrated the importance of wind forcing on river plume dynamics by combining numerical modeling results with remote sensing and *in situ* observations. Choi and Wilkin (2007) demonstrated the strong influence of buoyancy and wind forcing on the Hudson River plume. Similar findings were described for the Yukon River plume by Clark and Manzano (2022). The change of river plume direction caused by winds associated with the passage of low atmospheric pressure systems was investigated using the Navy Coastal Ocean Model (Cobb et al., 2008). The plume extension and orientation driven by the river discharge-wind interplay was described by Dong et al. (2004) for the Pearl River plume. An interesting model-

ing study showed the influence of Columbia River plume on the continental shelf during upwelling conditions, affecting the alongshore and cross-shore momentum transport as well as the vertical turbulence structure (Fulton, 2007). Normally, the river 50 plume flows northward along the Washington coast, but in spring-summer the upwelling-favorable winds and coastal circulation forces the plume farther south and offshore off Oregon (Hickey et al., 2005; Saldías et al., 2016). In general, the role of the wind forcing is enhanced on small river plumes (Osadchiev et al., 2021; Basdurak and Largier, 2022), which is the case for most river outflows along central-southern Chile (Saldías et al., 2016).

The relevance of combining hydrodynamic models with remote sensing and *in situ* data has been highlighted by Devlin 55 et al. (2015), who studied the river plumes on the Great Barrier Reef using MODIS imagery. In another study, Bai et al. (2010) used MERIS sensor data to characterize the Changjiang Estuary. In a recent study, Bainbridge et al. (2012) used MODIS images to describe the influence of river discharge, wind and Coriolis forcing on the Burdekin River plume and the transport of fine sediments and nutrients. In a study focused on Amur River, Abrosimova et al. (2009) compared direct observations with MODIS images and concluded that the plume is highly dynamic and is mostly controlled by the Earth's rotation in comparison 60 with the plume inertial effects.

Recent studies of river plumes off central Chile have been conducted using satellite imagery and numerical modeling results (Saldías et al., 2012, 2016; Salcedo-Castro et al., 2020; Rojas et al., 2023). These studies described a high seasonality in plume spreading and turbidity signals associated with the river discharge. In austral winter, a larger areal extent and the merging of the plumes can be observed after storms (coalescence events), whereas smaller plumes restricted to the nearfield region are 65 observed in austral spring-summer. A recent study combining remote sensing and numerical modeling results confirms that the river plumes and flow field are primarily modulated by the wind forcing in winter (Rojas et al., 2023). This work also highlights that the geostrophic component of the flow is associated with the wind modulation of the plume's shape on a synoptic scale.

This study aims to describe the interannual variability of the circulation and hydrographic conditions (and stratification) in the coastal area influenced by two rivers off central Chile: Maipo and Rapel rivers, complementing the previous study by 70 Salcedo-Castro et al. (2020) which was focused on the plume spreading climatology and vertical structure. To the best of our knowledge, this is the first interannual modeling study of these river plumes.

2 Methods

2.1 Study area

The study area, delimited by 32°30'S-34°S latitude, is representative of the Mediterranean climate of central Chile, where 75 the Maipo and Rapel rivers are discharged (Fig. 1). These are mixed rivers with snow- and rain-fed regimes, having higher discharges in winter and late spring. As most of Chilean rivers, they cover a relatively short distance across transverse and longitudinal valleys between the mountains and the coast, and have a small watershed (Saldías et al., 2012). However, their discharges are intervened by activities associated with mining, agriculture, industries and urban development, as there are several cities that account for a large population. The lower part of Rapel River is downstream of Rapel Dam, a reservoir

80 finished in 1968. In the lower coastal-estuarine region, the river discharges are under the influence of tides and local topography, characterized by a partially opened sandbar, with a strong seasonal wind influence (Flores et al., 2022).

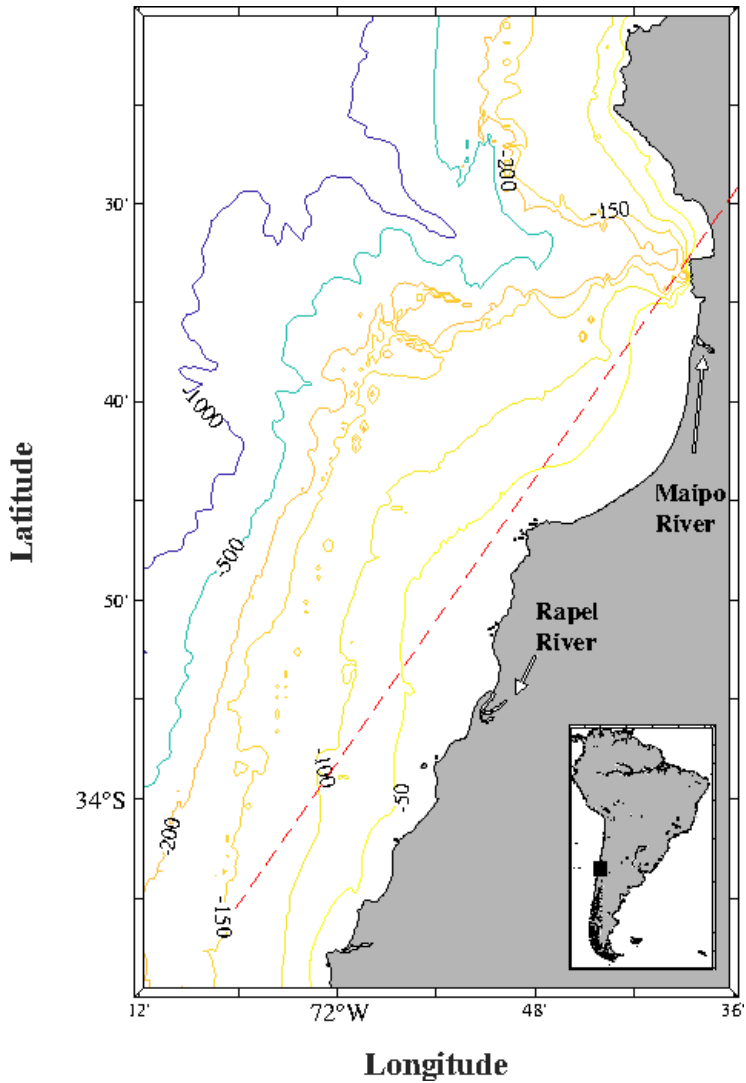


Figure 1. Study area showing Maipo and Rapel Rivers. The red dashed line represents the transect to describe the temporal variation of sea surface salinity (SSS) and vertical structure across the study area (see Fig. 9, Fig. 10 and Fig. 11).

2.2 Numerical model

We used the Coastal and Regional Ocean Community model (CROCO) and CROCO_TOOLS package (<http://www.croco-ocean.org>). This version solves the primitive hydrostatic equations of ocean dynamics, uses the terrain following coordinate and is

85 an adaptation of ROMS_AGRIF (Penven et al., 2006; Debreu et al., 2012), which is based on a new nonhydrostatic and a non-Boussinesq solver developed within the former ROMS kernel (Shchepetkin and McWilliams, 2005), for an optimal accuracy and cost efficiency (Hilt et al., 2020). The model was configured with a 1 km horizontal resolution (Arakawa C-grid) and 20 vertical levels, with higher resolution toward the surface and bottom levels. This configuration allows us to resolve submesoscale features of the river plumes and their interaction with mesoscale processes. The modeled period was 2003-2011.
 90 The model momentum and buoyancy fluxes were forced with the Scatterometer Climatology of Ocean Winds (SCOW) and the Comprehensive Ocean-Atmosphere Data Set (COADS), which have a 25 km resolution. Boundary conditions were obtained from the 10 km resolution Ocean General Circulation Model for the Earth Simulator (OFES), which was forced with fluxes from the National Centers for Environmental Prediction (NCEP). Daily river discharges from Maipo and Rapel rivers were obtained from the General Direction of Waters (Dirección General de Aguas, Chile) and complemented with the CAMELS-CL
 95 dataset (Alvarez-Garreton et al., 2018). The Rapel River gauge is located 25 km downstream of the dam and 16.5 km from the river mouth. The Maipo River gauge (Cabimba Station) is 21 km upstream from the river mouth. The monthly mean wind forcing and river discharges in the study area are shown in Fig. 2.

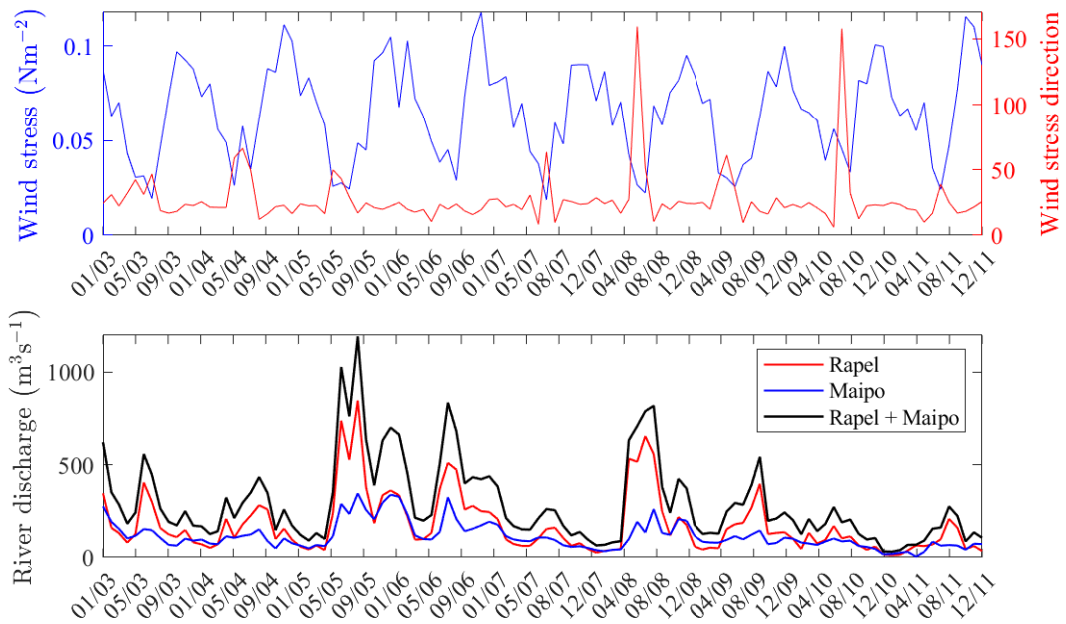


Figure 2. Monthly mean wind stress (OFES-NCEP) and river discharges (monthly averages) used to force the model in the study area.

The horizontal distribution of salinity was described to study the spatial-temporal variability of the plumes. A salinity value of 33.8 was used to delimit the plumes from ambient waters after computing monthly averages; this value is consistent with the
 100 reference value described by Rojas et al. (2023). To estimate the plume's area, a finer grid was generated by linear interpolation

and then exported as Geotiff images. These images were processed on ArcGIS Pro to measure the plume area and mean plume surface salinity (SSS).

Along with the description of salinity distribution, we also estimated the horizontal gradient of salinity (Yu, 2015; Freeman and Lovenduski, 2016; Saldías and Lara, 2020; Bao et al., 2021) as an indication of the strength of the plume's frontal characteristics. We computed the meridional and zonal gradients according to eqn. 1 and eqn. 2, which were combined to obtain the gradient magnitude at the center of each 1 km² grid cell (eqn. 3).

$$\text{Sgrad}_{(x)} = \frac{1}{2} \left(\frac{\text{S}_{(i+1,j)} - \text{S}_{(i,j)}}{\text{Lon}_{(i+1,j)} - \text{Lon}_{(i,j)}} + \frac{\text{S}_{(i+1,j+1)} - \text{S}_{(i,j+1)}}{\text{Lon}_{(i+1,j+1)} - \text{Lon}_{(i,j+1)}} \right) \quad (1)$$

$$\text{Sgrad}_{(y)} = \frac{1}{2} \left(\frac{\text{S}_{(i,j+1)} - \text{S}_{(i,j)}}{\text{Lat}_{(i,j+1)} - \text{Lat}_{(i,j)}} + \frac{\text{S}_{(i+1,j+1)} - \text{S}_{(i+1,j)}}{\text{Lat}_{(i+1,j+1)} - \text{Lat}_{(i,j)}} \right) \quad (2)$$

$$\text{Sgrad} = \sqrt{\text{Sgrad}_{(x)}^2 + \text{Sgrad}_{(y)}^2} \quad (3)$$

110 We used eqn. 4 to compute the area-averaged salinity gradient (AASG) in the whole domain (Salcedo-Castro et al., 2015).

$$\text{AASG} = \frac{1}{\text{Total area}} \sum_{i=1, j=1}^{i=m, j=n} \text{Sgrad}_{i,j} \times \text{Area}_{i,j} \quad (4)$$

The stratification in terms of the contribution by river discharges was assessed through the potential energy anomaly (PEA, J m⁻³) (Simpson et al., 1978; O'Donnell, 2010; Rojas et al., 2023) (eqn. 5):

$$\phi = \int_{-H}^{\eta} g(\rho - \bar{\rho}) z dz, \quad (5)$$

115 where the term $\bar{\rho}$ corresponds to the depth-averaged density (eqn. 6):

$$\bar{\rho} = \frac{1}{H} \int_{-H}^{\eta} \rho(z) dz, \quad (6)$$

We evaluated the PEA between 1 and 20 m along the transect depicted in Fig. 1 to represent the strength of stratification, as this represents the equivalent work to homogenize the water column (Simpson, 1981).

2.3 Empirical orthogonal functions (EOFs) and wavelet analysis

120 We performed an empirical orthogonal functions (EOF) analysis (Emery and Thomson, 2004) to the daily model outputs to evaluate the interannual variability of the plumes, reducing the dimensions of large datasets to a few significant orthogonal (uncorrelated) modes of variability and their associated time series (represented by the principal components (PC)). Considering that geophysical time series can be hard to be interpret because of the presence, even in the first modes, of complex

non-periodic signals (e.g. Olita et al. (2011a)), we analyzed the spectrum of the PCs by means of the continuous wavelet transform (CWT). The CWT allows the localization of a signal in the time domain neglecting some localization in frequency (Torrence and Compo, 1998). The rectification of the wavelet power spectra was calculated following Liu et al. (1998). We used the Morlet wavelet after removing the trends. Thus, spurious low-frequency signals are not considered in the analysis. The trend identification was performed by least squares linear fit.

3 Results

130 3.1 Horizontal plume pattern

The sea surface salinity (SSS), averaged over the 9-year period, and its standard deviation (STD) are shown in Fig. 3. The plumes are restricted to a relatively short area next to the river mouths and mostly oriented in the NW-NNW direction. This also reflects the mean direction of surface currents driven by northeasterward winds. The STD field reflects the largest variability associated with the lowest mean salinity near the river mouths – the plume's signal responds to the pulses of river discharges.

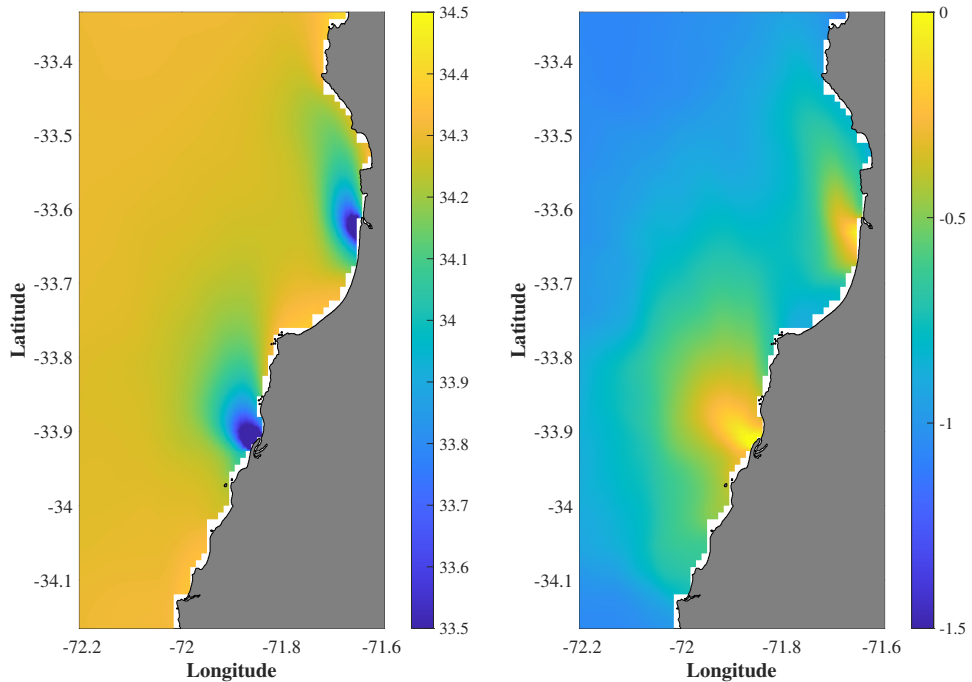


Figure 3. Maps of (left panel) averaged surface salinity over the 9 years period and (right panel) salinity standard deviation in logarithmic scale. Maximum variation of values is logically associated to the pulses river plume spreading.

135 The strong dependence of the plume horizontal pattern on the wind direction is especially evidenced during some winter months (Fig. 4), when wind is able to reverse the plume's northwestward direction. This is the situation observed in June 2008

and July 2010, corresponding to the two largest peaks observed in wind stress direction shown in Fig. 2. The plumes presented contrasting spreading in the coastal ocean, in response to the wind forcing; in winter 2008, the mean wind stress was 0.05 N m^{-2} , whereas the wind stress was predominantly 0.07 N m^{-2} in July 2010.

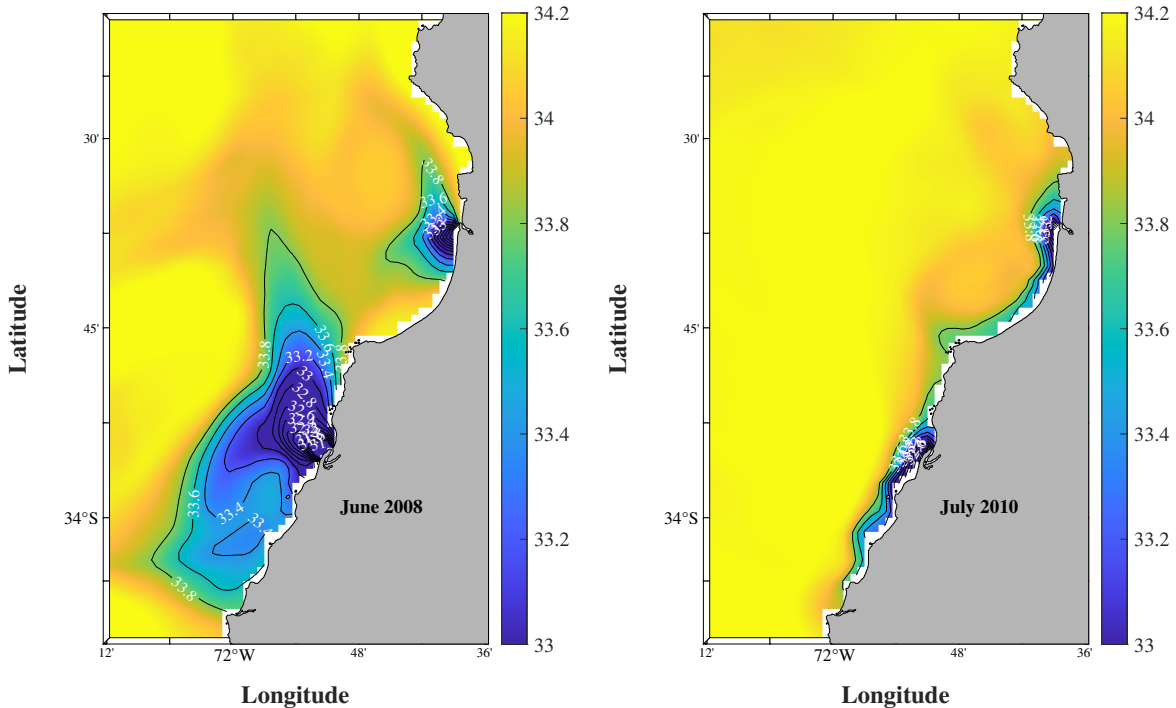


Figure 4. Salinity distribution in June 2008 and July 2010, corresponding to the changes in wind stress direction to SSE – see Fig. 2.

140 We defined the limit of the plume's area with a salinity value of 33.8 in order to separate the plumes from ambient waters. This value was chosen as representative after exploring the statistical distribution of salinity over the entire period; other authors have other criteria, depending on the objectives of the study and the dynamic characteristics of the area under study (Falcieri et al., 2014). The variation of the plume area (< 33.8), total river discharge (Maipo + Rapel) and mean surface salinity is shown in Fig. 5. where it is possible to see a direct and inverse relationship, respectively. These relationships are clearly observed in 145 Fig. 6.

The minimum and maximum salinity in the domain shows a clear increasing salinity trend over the entire period Fig. 7, which is related to a gradual decrease in river discharge. The interannual variability revealed major plume events with reduced salinity during the winters of 2005 and 2008.

150 The variation of the strength of the area-averaged salinity gradient (AASG) (Fig. 8) is consistent with the extension of the plumes and correlates with the total river discharges (Fig. 5), which involves stronger gradients and fronts during fall-winter.

Besides the variation in the total area, the alongshore extension was also evaluated in order to identify interannual variability of plume influence along the coast (Fig. 1). Episodes of high river discharges are normally accompanied by an extension of up

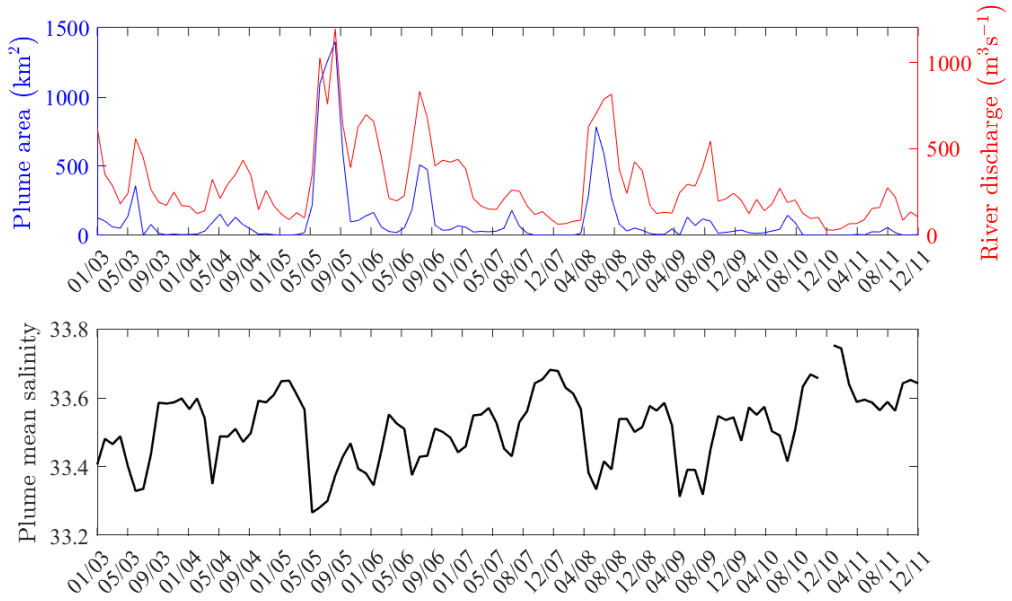


Figure 5. Variation of (upper panel) river plume area and total river discharge, and (lower panel) mean plume salinity for the period 2003–2011.

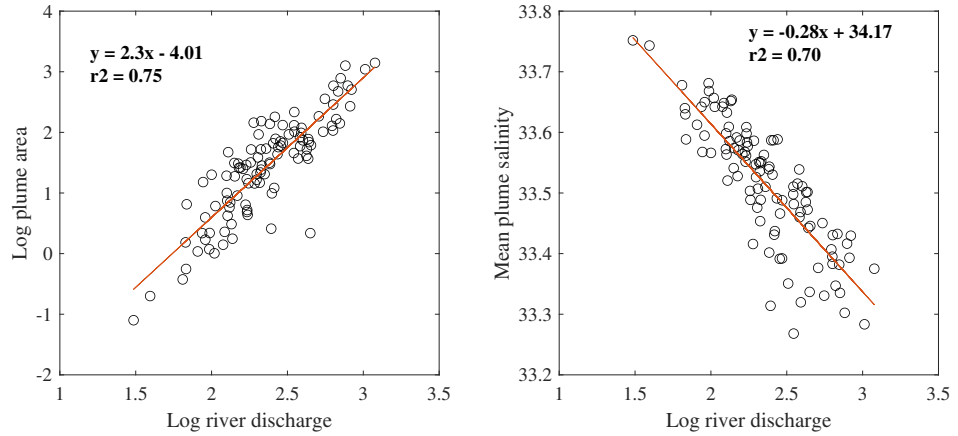


Figure 6. Scatter plot of (left panel) river plume area and (right panel) mean plume salinity as function of total river discharge.

to 30 km southward along the coast and coalescence of the plumes (Fig. 9), which is consistent with changes in wind direction (Fig. 2 and Fig. 4). The years 2005, 2006 and 2008 presented a marked plume extension during austral winter, whereas the 155 summers of years 2005, 2007 and 2010 were characterized by a minimum or absence of the plumes along the entire coast.

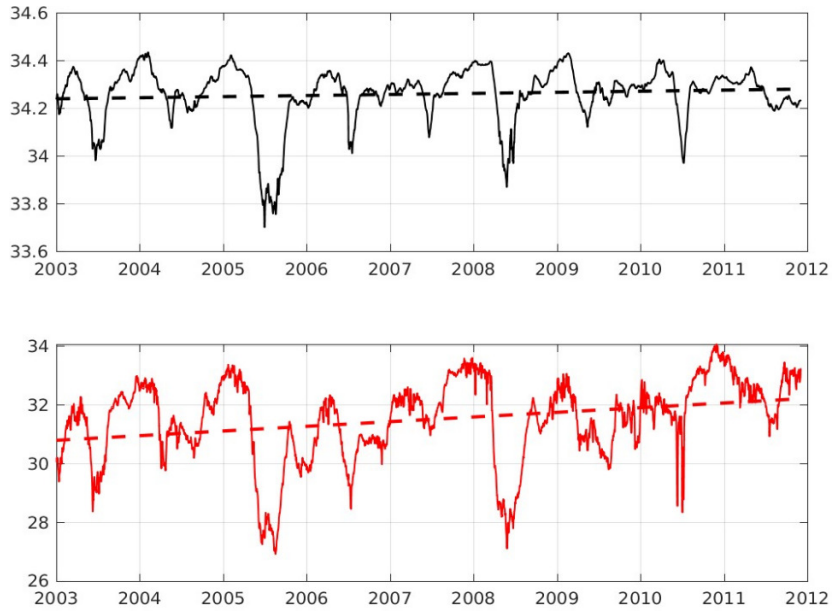


Figure 7. Time series and trends of the (top panel) maximum and (bottom panel) minimum surface salinity over the domain

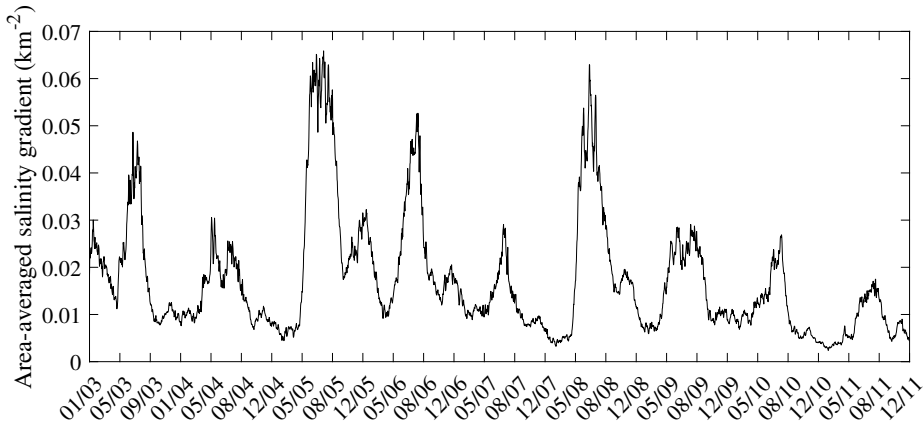


Figure 8. Variation of the area-averaged salinity gradient (AASG) in the Maipo-Rapel plume area.

3.2 Vertical plume pattern

The effect of river discharges on the vertical distribution of salinity along the longitudinal transect (Fig. 1) is shown in Fig. 10. We can observe that both plumes can distribute individually and there are episodes of coalescence, especially during high river discharges. Also, during some summer-fall months the plumes are so reduced that they are not detected along this transect. If

160 we use a salinity of 34.2 as a vertical boundary value, the plume thickness increased up to 15 m during high river discharge

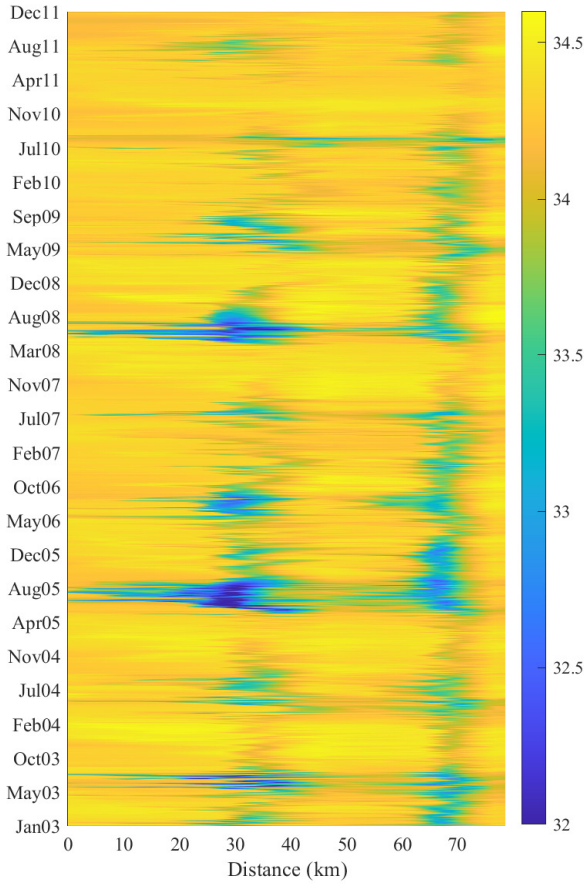


Figure 9. Hovmöller diagram for sea surface salinity (SSS) along a longitudinal transect (see Fig. 1) extending across Maipo and Rapel river plumes.

events. These events also involve a stronger stratification. The time variation along the longitudinal transect of stratification strength (Fig. 11), represented by the potential energy anomaly (PEA, J m^{-3}), agrees with variations of sea surface salinity (Fig. 9) and river discharges (Fig. 5).

3.3 EOFs and wavelet

165 Here following are presented the first 3 modes of variability (Fig. 12 to Fig. 14). Results are presented as follows: a map representing the EOF mode, thus, below, the EOF expansion coefficient (PC time series) with the related wavelet power spectrum and, on the right, the cumulative wavelet spectrum. The first 4 modes of variability explain the 66.7, 9.1, 5.5, 4.9 of

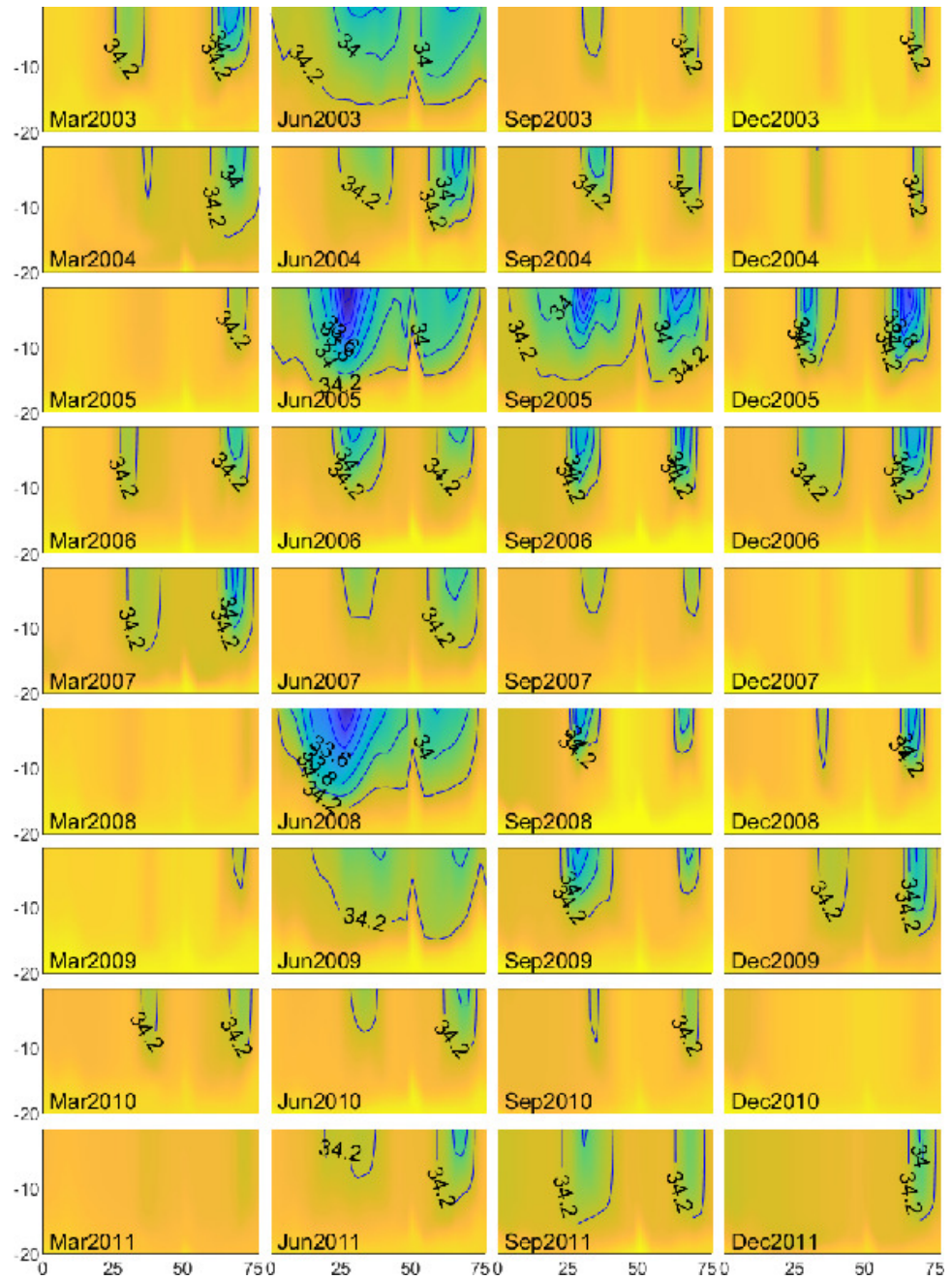


Figure 10. Vertical distribution of salinity along the longitudinal transect (Fig. 1) in the Maipo-Rapel River plumes area.

variability, respectively. The first mode explains the seasonal variability, as it can clearly be deduced by observing the related

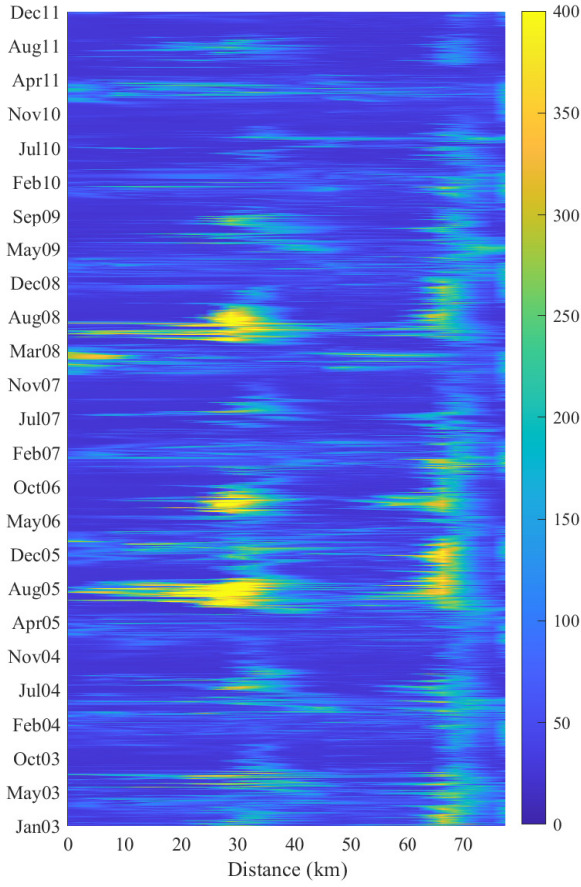


Figure 11. Hovmöller diagram for potential energy anomaly (PEA, J m^{-3}) along the longitudinal transect (see Fig. 1) extending across Maipo and Rapel river plumes.

PC and its wavelet decomposition. The whole domain is in phase in this mode of variability, i.e. the system variability varies
170 in the same direction (Fig. 12).

In the second mode we can observe an interesting feature, probably related to meteorological events. Here, the time series shows an high frequency signature, with two distinct and relevant events, having a period of few months, centered in 2005 and 2010, that are probably related to particular drought events. This feature is of interest also looking at the spatial counter-phase character, as the southernmost area of the domain shows a different sign with respect to the estuaries area. The shape of the
175 southern plume forms a front with a southern area having a positive sign. This could be linked to a low-precipitations mode that reduces the area of influence of the estuaries with their plume, with special reference to the southern one (Fig. 13). Also the

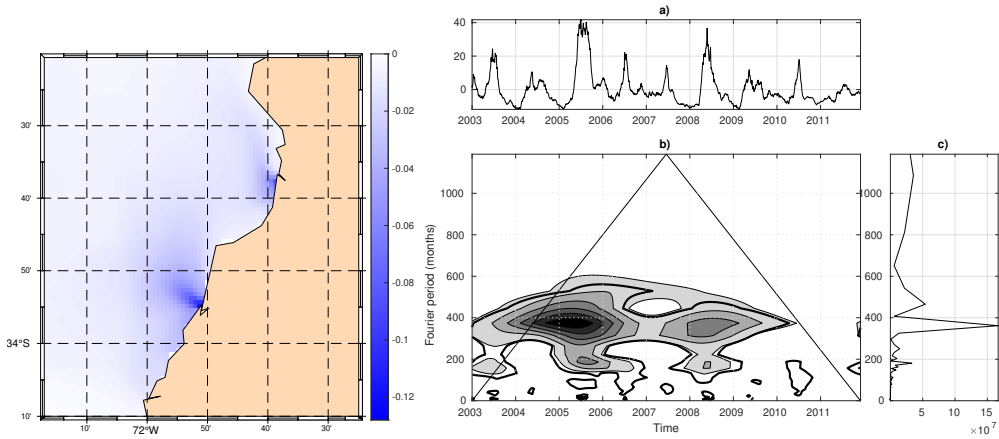


Figure 12. (Left panel) EOF Mode 1 map. (a) EOF PC 1 time series, (b) Wavelet spectrum of the PC series and (c) cumulative global wavelet spectrum.

direction of the plumes for this mode of variability seems to be northward more than the usual climatological NW direction. This could be related to changes in wind direction and intensity for this two particular events.

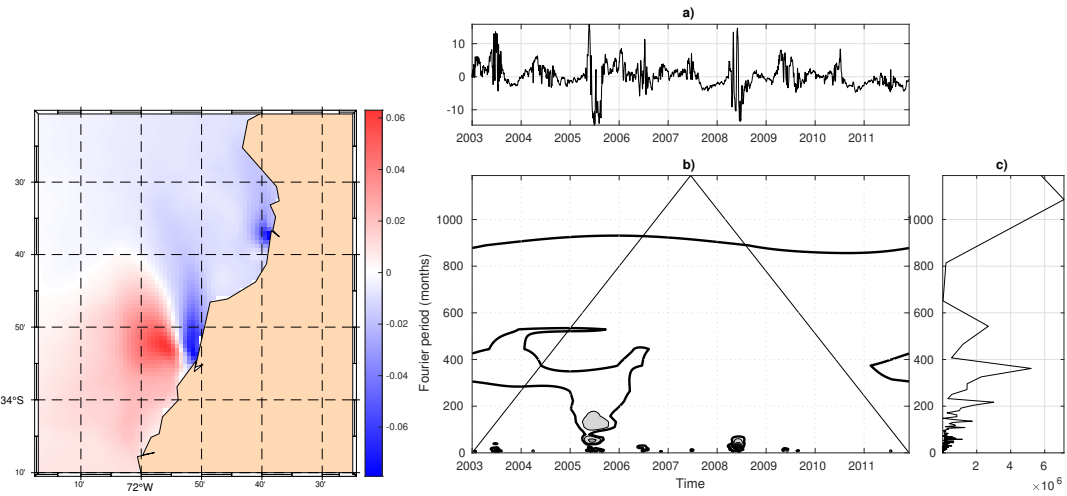


Figure 13. (Left panel) EOF Mode 2 map. (a) EOF PC 2 time series, (b) Wavelet spectrum of the PC series and (c) cumulative global wavelet spectrum.

The third mode is related again to a high frequency, probably mesoscale-related, signal superimposed on a longer signal
180 at the end of the series. This corresponds to a reduction of this signature of the plumes, where high frequency signature characterize a longer-period signal probably related to the beginning of the 2010-2015 mega-drought (Fig. 14). Other higher

modes of variability are more difficult to be interpreted and are not presented in this analysis, as they could also be related to non-physical features. The most noticeable events are those shown in the second mode of variability. This feature in the spatial mode corresponds to two distinct minima of surface salinity related, especially to the Rapel River plume.

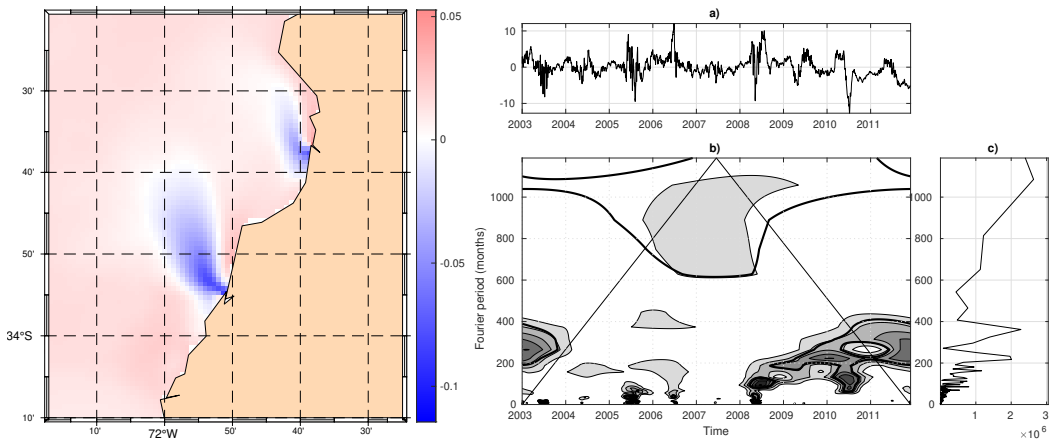


Figure 14. (Left panel) EOF Mode 3 map. (a) EOF PC 3 time series, (b) Wavelet spectrum of the PC series and (c) cumulative global wavelet spectrum.

185 4 Discussion

During the 9-years period, it can be observed that the river plumes are normally restricted to a short distance from the river mouth, where they also exhibit larger horizontal variability, although there is a more uniform condition vertically close to the river mouth. In an analytical study, Hetland (2005) stated that mixing is more intense near the river mouth while wind efficiency is higher far from the river mouth, which is consistent with the plume shape and orientation. Similarly, other authors 190 have pointed out that in the near field the plume behaves as a buoyant jet with stronger effect of the bottom, while in the far field the horizontal density gradient is weaker and strongly affected by wind and Coriolis force (Chao, 1988; Chen et al., 2009; Horner-Devine et al., 2015). In our study, we can observe a strongly stratified plume even in the far field during winter months; this contrast is explained by the combination of larger river discharge and weaker wind efficiency.

Considering their relatively steep slopes and small watersheds, compared to larger rivers, Maipo and Rapel rivers are similar 195 to systems that exhibit a rapid response to episodes of increase in freshwater, generating river plumes with a strong stratification within 1 km of the river mouth (Warrick et al., 2004). An interesting feature observed in river plumes is the occurrence of "rooted" plumes in shallow areas (Zhi et al., 2022). It is possible that this process can also occur in central Chile, especially, under the influence of northwesterly winds in winter.

The plume extension and mean surface salinity is strongly correlated with the river discharge, with wind playing a secondary 200 role mostly influencing the plume shape and orientation, as observed during two winter episodes with northwesterly winds also

described elsewhere by Rojas et al. (2023). Comparing different forcing, Hickey et al. (2005) state that the extension and shape of the river plumes mostly depend on river runoff, wind and surface currents over the continental shelf. Although there are other factors that influence the spread of a river discharge, like tides, characteristics of the discharge, bathymetry, and Coriolis acceleration (Archetti and Mancini, 2012). For instance, Chen et al. (2017a) state that, outside the micro-tidal estuary, wind 205 is the main forcing contributing energy for mixing the Pearl River plume over the shelf. This explains the vertical pattern observed in the Maipo-Rapel river area, in agreement with Rojas et al. (2023), where the higher PEA and stratification are observed in winter, when wind is weaker and river discharge is the most important driver of the plume dynamics, except during the northwesterly wind events.

Fernández-Nóvoa et al. (2015) showed that the river discharge had a higher variability during the period of higher discharge 210 and when landward, downwelling-favorable winds pushed the plume to the coast, making it flow along the coast. Something similar is observed during episodes of strong NNW winds off Maipo-Rapel rivers occurring in winter. This seasonal change in the plume extension and direction had already been described by other authors (Fiedler and Laurs, 1990; García Berdeal et al., 2002).

Subtidal currents associated with wind-influenced currents and mesoscale eddies are also an important forcing linked to the 215 transport of river plume sediment over long distances and long time scales (Blaas et al., 2007). However, the intra-annual and seasonal variability remain driven by wind and river discharges, respectively, as it has also been observed in other systems where river discharge controls the plume dynamics in the long term while wind is more relevant in the short term (Falcieri et al., 2014). In this sense, consistent with our results, Piñones et al. (2005), assert that the Maipo River plume is mostly driven by the river discharge in winter but the influence of wind is more important during spring-summer. Normally, the predominant 220 wind in this region is from southwest, decreasing its intensity in fall-winter (Strub et al., 1998) and with episodic strong storms during winter (Hernández-Miranda et al., 2003) and periods of upwelling and relaxation and intrusion of oceanic waters during summer (Letelier et al., 2009; Aguirre et al., 2012).

We compared the model results with El Niño-Southern Oscillation (ENSO) and Pacific Interdecadal Oscillation (PDO) indices: in both cases no significant correlation was found. In this sense, Hernandez et al. (2022) pointed out that, even though 225 some catchments are strongly correlated ENSO with related hydro-climatic anomalies, mixed regimes do not exhibit a clear connection. On the other hand, Alvarez-Garreton et al. (2021) stated that snow-dominated catchments are especially vulnerable to long term droughts, showing the accumulated effect from previous years; this could be reflected especially in a reduction of the plumes extension during spring-summer, as observed after 2008 (Fig. 5). This long-term drought has been described by other authors (Winckler et al., 2020), which is attributed to the anthropogenic climate change, with an evident decrease in river 230 discharges in central Chile since 2010.

The pattern here described is opposite to the interannual and seasonal variability of the Columbia River. Here, Burla et al. (2010) and Chen et al. (2017a) described a northward plume attached to the coast in winter and a detached plume in summer, detaching that is normally observed during events of wind relaxation or wind reversal. Moreover, Chen et al. (2017b) asserted that upwelling jets are able to transport river plumes long distances along the coast. However, whereas Columbia River 235 has a snow-dominated regime where a maximum river discharge coincides with the period of intense upwelling-favorable

winds, river plumes in central Chile are characterized by a phase difference between higher freshwater discharge and stronger upwelling-favorable winds. The detachment of the plumes (northwestward direction) observed during summer in this study is in agreement with the Ekman theory, as described by Rojas et al. (2023) and Saldías et al. (2012), where upwelling-favorable wind forces the detachment and direction of the buoyancy-driven plume.

240 An interesting point to consider is the conclusion by Berghuijs et al. (2014), who state that a shift from snow- to rain-dominated regimes in some catchments would lead to a decrease in the mean streamflow. In pluvio-nival regimes like Rapel and Maipo rivers, this would mean that plumes extending on coastal areas would mostly depend on the river discharges occurring in winter. In this sense, Döll and Schmied (2012) modeled climate change projections and asserted that some specific river flow indicators might change; for instance, low flows could decrease up to 50% some systems could change their regime from 245 perennial to intermittent.

As described by Garreaud and Falvey (2009), it is expected that future conditions in this region will be characterized by stronger southerly winds, which would involve that Rapel and Maipo rivers could extend further north and closer to the coast. On the other hand, projections also predict a southward extension of the semi-arid climate (Winckler et al., 2020), which means that the river discharges in this region would tend to decrease over time. Thus, we would expect smaller river plumes which 250 would extend closer to the coast and probably have so impact on the distribution of benthic communities and larval stages (Grimes and Kingsford, 1996), besides a strong impact in sand supply to beaches that strongly depend on these rivers and that already show a progressive erosion and shoreline retreat (Martínez et al., 2018, 2022). Although not explored in this study, it is evident that ENSO hydro-climatic anomalies have a strong influence on the hydrological regime (Hernandez et al., 2022) and plume structure along central-south Chilean coasts, depending on the latitude (Saldías et al., 2016). Consequently, it is 255 expected to observe changes in the pattern described here during the coming decades.

Although the model does not include the wave effect, further studies should consider this variable as most of the plume remains attached to the coasts, especially, during high-energy wave events in winter. In this sense, Delpay et al. (2014) describes the strong effect that waves can have on the river plume dynamics, including alongshore currents and flushing time. A recent study on Maipo River plume also demonstrates the strong influence that waves can have on plume dynamics on shallow areas 260 (Flores et al., 2022).

5 Conclusions

The hydrography of the area influenced by Maipo and Rapel River plumes was modelled for the period 2003-2011, where a strong dependence of the plumes features on freshwater discharge and wind forcing could be evidenced. Unlike other systems like Columbia River, the larger extent, lower mean salinity and stronger stratification is observed in winter time, when wind 265 is weaker and some times downwelling-favorable; in spring-summer, when upwelling-favorable wind is stronger, these river plumes are smaller and their stratification is weaker, which is consistent with previous studies. Strong, downwelling-favorable, events are able to reverse the river plume direction and push it southward to form a narrow band attached to the coast. The

EOFs analysis confirmed the strong seasonality of the Maipo-Rapel river plume system. A second mode showed an intra-annual signal, likely associated with meteorological events, which also exhibited a contrasting north-south spatial sign.

270 An increasing trend of mean salinity was observed in the study domain, associated with a decreasing trend in river discharges. This trend corresponds to the beginning of the 2010-2015 mega-drought exhibited by this region. No correlation was found between the plumes characteristics and El Niño-Southern Oscillation (ENSO) and Pacific Interdecadal Oscillation (PDO) indices, which would be explained by the complexity of mixed regimes and the fact that snow melting regimes show a lag and cumulative response from previous years. It is possible to speculate that a shift from snow- to rain-dominated regimes, along 275 with changes in wind and precipitation patterns will be reflected on smaller river plumes and more attached to the coast, along with an increase in local mean surface salinity, which would affect planktonic and benthic communities.

Author contributions. TEXT

280 JSC ellaborated the idea and general organization of the manuscript; AO undertook the EOF and wavelets analyses along with the respective discussion. FS contributed to the remote sensing review, analyses, and discussion. MC carried out the vertical structure analysis and discussion. GS and RCG collaborated with the manuscript organization, edition and discussions.

Competing interests. TEXT

No competing interests are present.

Disclaimer. TEXT

285 Acknowledgements. This study was funded by CONICYT FONDECYT Chile, grant 11160309 “Numerical modeling of river plumes in central Chile (32S-34S) and assessment of climate change scenarios” and the Millennium Nucleus Center for the Study of Multiple Drivers on Marine Socio-Ecological Systems funded by MINECON, Chile NC120028.

References

Abrosimova, A., Zhabin, I., and Dubina, V.: Influence of the Amur River runoff on the hydrological conditions of the Amur Liman and Sakhalin Bay (Sea of Okhotsk) during the spring-summer flood, Tech. rep., V.I. Il'ichev Pacific Oceanological Institute, FEB RAS, 290 Vladivostok, Russia, <https://doi.org/10.3103/S1068373910040084>, 2009.

Acker, J. G., McMahon, E., Shen, S., Hearty, T., and Casey, N.: Time-series analysis of remotely-sensed SeaWiFS chlorophyll in river-influenced coastal regions, in: EARSeL eProceedings, 8(2), pp. 114–139, 2009.

Aguirre, C., Pizarro, Ó., Strub, P. T., Garreaud, R., and Barth, J. A.: Seasonal dynamics of the near-surface alongshore flow off central Chile, *Journal of Geophysical Research: Oceans*, 117, <https://doi.org/10.1029/2011JC007379>, 2012.

295 Alvarez-Garreton, C., Mendoza, P. A., Pablo Boisier, J., Addor, N., Galleguillos, M., Zambrano-Bigiarini, M., Lara, A., Puelma, C., Cortes, G., Garreaud, R., McPhee, J., and Ayala, A.: The CAMELS-CL dataset: Catchment attributes and meteorology for large sample studies-Chile dataset, *Hydrology and Earth System Sciences*, 22, 5817–5846, <https://doi.org/10.5194/hess-22-5817-2018>, 2018.

Alvarez-Garreton, C., Pablo Boisier, J., Garreaud, R., Seibert, J., and Vis, M.: Progressive water deficits during multiyear droughts in basins with long hydrological memory in Chile, *Hydrology and Earth System Sciences*, 25, 429–446, <https://doi.org/10.5194/hess-25-429-2021>, 300 2021.

Archetti, R. and Mancini, M.: Freshwater dispersion plume in the sea: Dynamic description and case study, in: *Hydrodynamics - Natural Water Bodies*, edited by Schulz, H. E., Simoes, A. L. A., and Lobosco, R. J., IntechOpen, London, <https://doi.org/10.5772/28390>, 2012.

Bai, Y., He, X., Pan, D., Zhu, Q., Lei, H., Tao, B., and Hao, Z.: The extremely high concentration of suspended particulate matter in Changjiang Estuary detected by MERIS data, in: *Remote Sensing of the Coastal Ocean, Land, and Atmosphere Environment*, vol. 7858, 305 p. 78581D, SPIE, <https://doi.org/10.1117/12.869632>, 2010.

Bainbridge, Z. T., Wolanski, E., Álvarez-Romero, J. G., Lewis, S. E., and Brodie, J. E.: Fine sediment and nutrient dynamics related to particle size and floc formation in a Burdekin River flood plume, Australia, *Marine Pollution Bulletin*, 65, 236–248, <https://doi.org/10.1016/j.marpolbul.2012.01.043>, 2012.

Bao, S., Wang, H., Zhang, R., Yan, H., Chen, J., and Bai, C.: Application of Phenomena-Resolving Assessment Methods to Satellite Sea 310 Surface Salinity Products, *Earth and Space Science*, 8, 1–14, <https://doi.org/10.1029/2020EA001410>, 2021.

Basdurak, N. and Largier, J.: Wind Effects on Small-Scale River and Creek Plumes, *Journal of Geophysical Research: Oceans*, p. e2021JC018381, 2022.

Berghuijs, W. R., Woods, R. A., and Hrachowitz, M.: A precipitation shift from snow towards rain leads to a decrease in streamflow, *Nature Climate Change*, 4, 583–586, <https://doi.org/10.1038/nclimate2246>, 2014.

315 Blaas, M., Dong, C., Marchesiello, P., McWilliams, J. C., and Stolzenbach, K. D.: Sediment-transport modeling on Southern Californian shelves: A ROMS case study, *Continental Shelf Research*, 27, 832–853, <https://doi.org/10.1016/j.csr.2006.12.003>, 2007.

Bloodsworth, K. H., Tilburg, C. E., and Yund, P. O.: Influence of a River Plume on the Distribution of Brachyuran Crab and Mytilid Bivalve Larvae in Saco Bay, Maine, *Estuaries and Coasts*, 38, 1951–1964, <https://doi.org/10.1007/s12237-015-9951-5>, 2015.

Burla, M., Baptista, A. M., Zhang, Y., and Frolov, S.: Seasonal and interannual variability of the Columbia River plume: A perspective 320 enabled by multiyear simulation databases, *Journal of Geophysical Research*, 115, <https://doi.org/10.1029/2008JC004964>, 2010.

Carreon-Martinez, L. B., Wellband, K. W., Johnson, T. B., Ludsin, S. A., and Heath, D. D.: Novel molecular approach demonstrates that turbid river plumes reduce predation mortality on larval fish, *Molecular Ecology*, 23, 5366–5377, <https://doi.org/10.1111/mec.12927>, 2014.

Chakraborty, S. and Lohrenz, S. E.: Phytoplankton community structure in the river-influenced continental margin of the northern Gulf of 325 Mexico, *Marine Ecology Progress Series*, 521, 31–47, <https://doi.org/10.3354/meps11107>, 2015.

Chao, S.-Y.: River-forced estuarine plumes, *Journal of Physical Oceanography*, 18, 72–88, 1988.

Chen, F., MacDonald, D. G., and Hetland, R. D.: Lateral spreading of a near-field river plume: Observations and numerical simulations, 330 *Journal of Geophysical Research: Oceans*, 114, <https://doi.org/10.1029/2008JC004893>, 2009.

Chen, Z., Gong, W., Cai, H., Chen, Y., and Zhang, H.: Dispersal of the Pearl River plume over continental shelf in summer, *Estuarine, Coastal 335 and Shelf Science*, 194, 252–262, <https://doi.org/10.1016/j.ecss.2017.06.025>, 2017a.

Chen, Z., Pan, J., Jiang, Y., and Lin, H.: Far-reaching transport of Pearl River plume water by upwelling jet in the northeastern South China 340 Sea, *Journal of Marine Systems*, 173, 60–69, <https://doi.org/10.1016/j.jmarsys.2017.04.008>, 2017b.

Choi, B. J. and Wilkin, J. L.: The effect of wind on the dispersal of the Hudson River plume, *Journal of Physical Oceanography*, 37, 1878–1897, <https://doi.org/10.1175/JPO3081.1>, 2007.

345 Clark, J. B. and Mannino, A.: The Impacts of Freshwater Input and Surface Wind Velocity on the Strength and Extent of a Large High Latitude River Plume, *Frontiers in Marine Science*, 8, <https://doi.org/10.3389/fmars.2021.793217>, 2022.

Cobb, M., Keen, T. R., and Walker, N. D.: Modeling the circulation of the Atchafalaya Bay system. Part 2: River plume dynamics during cold fronts, *Journal of Coastal Research*, 24, 1048–1062, <https://doi.org/10.2112/07-0879.1>, 2008.

350 Debreu, L., Marchesiello, P., Penven, P., and Cambon, G.: Two-way nesting in split-explicit ocean models: Algorithms, implementation and validation, *Ocean Modelling*, 49–50, 1–21, <https://doi.org/10.1016/j.ocemod.2012.03.003>, 2012.

Delpay, M. T., Ardhuin, F., Otheguy, P., and Jouon, A.: Effects of waves on coastal water dispersion in a small estuarine bay, *Journal of Geophysical Research: Oceans*, 119, 70–86, <https://doi.org/10.1002/2013JC009466>, 2014.

355 Devlin, M. J., Petus, C., da Silva, E., Tracey, D., Wolff, N. H., Waterhouse, J., and Brodie, J.: Water quality and river plume monitoring in the Great Barrier Reef: An overview of methods based on ocean colour satellite data, *Remote Sensing*, 7, 12 909–12 941, <https://doi.org/10.3390/rs71012909>, 2015.

Döll, P. and Schmied, H. M.: How is the impact of climate change on river flow regimes related to the impact on mean annual runoff? A global-scale analysis, *Environmental Research Letters*, 7, <https://doi.org/10.1088/1748-9326/7/1/014037>, 2012.

360 Dong, L., Su, J., Ah Wong, L., Cao, Z., and Chen, J. C.: Seasonal variation and dynamics of the Pearl River plume, *Continental Shelf Research*, 24, 1761–1777, <https://doi.org/10.1016/j.csr.2004.06.006>, 2004.

D'sa, E. J. and Miller, R. L.: Bio-optical properties in waters influenced by the Mississippi River during low flow conditions, *Remote Sensing of Environment*, 84, 538–549, www.elsevier.com/locate/rse, 2003.

365 Emery, W. J. and Thomson, R. E.: *Data Analysis Methods in Physical Oceanography*, Elsevier, Amsterdam, 2nd edn., 2004.

Falcieri, F. M., Benetazzo, A., Sclavo, M., Russo, A., and Carniel, S.: Po River plume pattern variability investigated from model data, *Continental Shelf Research*, 87, 84–95, <https://doi.org/10.1016/j.csr.2013.11.001>, 2014.

370 Fan, Y., Zhang, S., Du, X., Wang, G., Yu, S., Dou, S., Chen, S., Ji, H., Li, P., and Liu, F.: The effects of flow pulses on river plumes in the Yellow River Estuary, in spring, *Journal of Hydroinformatics*, 00, 1–15, <https://doi.org/10.2166/hydro.2022.049>, 2022.

Fernández-Nóvoa, D., Mendes, R., DeCastro, M., Dias, J. M., Sánchez-Arcilla, A., and Gómez-Gesteira, M.: Analysis of the influence of river discharge and wind on the Ebro turbid plume using MODIS-Aqua and MODIS-Terra data, *Journal of Marine Systems*, 142, 40–46, <https://doi.org/10.1016/j.jmarsys.2014.09.009>, 2015.

375 Fiedler, P. C. and Laurs, R. M.: Variability of the Columbia River plume observed in visible and infrared satellite imagery, *International Journal of Remote Sensing*, 11, 999–1010, 1990.

Flores, R. P., Williams, M. E., and Horner-Devine, A. R.: River Plume Modulation by Infragravity Wave Forcing, *Geophysical Research Letters*, 49, <https://doi.org/10.1029/2021GL097467>, 2022.

Fong, D. A. and Rockwell Geyer, W.: Response of a river plume during an upwelling favorable wind event, *Journal of Geophysical Research: Oceans*, 106, 1067–1084, <https://doi.org/10.1029/2000JC900134>, 2001.

365 Forrest, B. M., Gillespie, P. A., Cornelisen, C. D., and Rogers, K. M.: Multiple indicators reveal river plume influence on sediments and benthos in a New Zealand coastal embayment, *New Zealand Journal of Marine and Freshwater Research*, 41, 13–24, 2007.

Freeman, N. M. and Lovenduski, N. S.: Mapping the Antarctic Polar Front: Weekly realizations from 2002 to 2014, *Earth System Science Data*, 8, 191–198, <https://doi.org/10.5194/essd-8-191-2016>, 2016.

370 Fulton, D. P.: Modeling the Columbia River Plume on the Oregon Shelf during Summer Upwelling, Tech. rep., Cooperative Institute for Oceanographic Satellite Studies, <http://www.orcoos.org>, 2007.

García Berdeal, I., Hickey, B. M., and Kawase, M.: Influence of wind stress and ambient flow on a high discharge river plume, *Journal of Geophysical Research: Oceans*, 107, <https://doi.org/10.1029/2001jc000932>, 2002.

Garreaud, R. D. and Falvey, M.: The coastal winds off western subtropical South America in future climate scenarios, *International Journal of Climatology*, 29, 543–554, <https://doi.org/10.1002/joc.1716>, 2009.

375 Grimes, C. B. and Kingsford, M. J.: How do riverine plumes of different sizes influence fish larvae: do they enhance recruitment?, *Marine and Freshwater Research*, 47, 191–208, 1996.

Hernandez, D., Mendoza, P. A., Boisier, J. P., and Ricchetti, F.: Hydrologic Sensitivities and ENSO Variability Across Hydrological Regimes in Central Chile (28°–41°S), *Water Resources Research*, 58, <https://doi.org/10.1029/2021wr031860>, 2022.

380 Hernández-Miranda, E., Palma, A. T., and Ojeda, F. P.: Larval fish assemblages in nearshore coastal waters off central Chile: Temporal and spatial patterns, *Estuarine, Coastal and Shelf Science*, 56, 1075–1092, [https://doi.org/10.1016/S0272-7714\(02\)00308-6](https://doi.org/10.1016/S0272-7714(02)00308-6), 2003.

Hetland, R. D.: Relating river plume structure to vertical mixing, *Journal of Physical Oceanography*, 35, 1667–1688, 2005.

Hetland, R. D.: The effects of mixing and spreading on density in near-field river plumes, *Dynamics of Atmospheres and Oceans*, 49, 37–53, <https://doi.org/10.1016/j.dynatmoce.2008.11.003>, 2010.

385 Hickey, B., Geier, S., Kachel, N., and MacFadyen, A.: A bi-directional river plume: The Columbia in summer, *Continental Shelf Research*, 25, 1631–1656, <https://doi.org/10.1016/j.csr.2005.04.010>, 2005.

Hilt, M., Auclair, F., Benshila, R., Bordois, L., Capet, X., Debret, L., Dumas, F., Jullien, S., Lemarié, F., Marchesiello, P., Nguyen, C., and Roblou, L.: Numerical modelling of hydraulic control, solitary waves and primary instabilities in the Strait of Gibraltar, *Ocean Modelling*, 151, <https://doi.org/10.1016/j.ocemod.2020.101642>, 2020.

390 Horner-Devine, A. R., Hetland, R. D., and MacDonald, D. G.: Mixing and transport in coastal river plumes, <https://doi.org/10.1146/annurev-fluid-010313-141408>, 2015.

Kudela, R. M. and Peterson, T. D.: Influence of a buoyant river plume on phytoplankton nutrient dynamics: What controls standing stocks and productivity?, *Journal of Geophysical Research: Oceans*, 114, <https://doi.org/10.1029/2008JC004913>, 2009.

Lentz, S. J. and Largier, J.: The influence of wind forcing on the Chesapeake Bay buoyant coastal current, *Journal of Physical Oceanography*, 36, 1305–1316, 2006.

395 Letelier, J., Pizarro, O., and Nuñez, S.: Seasonal variability of coastal upwelling and the upwelling front off central Chile, *Journal of Geophysical Research: Oceans*, 114, <https://doi.org/10.1029/2008JC005171>, 2009.

Liu, W. T., Tang, W., and Polito, P. S.: NASA scatterometer provides global ocean-surface wind fields with more structures than numerical weather prediction, *Geophysical Research Letters*, 25, 761, <https://doi.org/10.1029/98GL00544>, 1998.

400 Mallin, M. A., Cahoon, L. B., and Durako, M. J.: Contrasting food-web support bases for adjoining river-influenced and non-river influenced continental shelf ecosystems, *Estuarine, Coastal and Shelf Science*, 62, 55–62, <https://doi.org/10.1016/j.ecss.2004.08.006>, 2005.

Martínez, C., Contreras-López, M., Winckler, P., Hidalgo, H., Godoy, E., and Agredano, R.: Coastal erosion in central Chile: A new hazard?, *Ocean and Coastal Management*, 156, 141–155, <https://doi.org/10.1016/j.ocecoaman.2017.07.011>, 2018.

Martínez, C., Grez, P. W., Martín, R. A., Acuña, C. E., Torres, I., and Contreras-López, M.: Coastal erosion in sandy beaches along a tectonically active coast: The Chile study case, *Progress in Physical Geography*, 46, 250–271, <https://doi.org/10.1177/03091333211057194>, 2022.

Masotti, I., Aparicio-Rizzo, P., Yevenes, M. A., Garreaud, R., Belmar, L., and Farías, L.: The influence of river discharge on nutrient export and phytoplankton biomass off the Central Chile Coast (33°–37°S): Seasonal cycle and interannual variability, *Frontiers in Marine Science*, 5, <https://doi.org/10.3389/fmars.2018.00423>, 2018.

410 Mestres, M., Sierra, J. P., Sánchez-Arcilla, A., González del Río, J., Wolf, T., Rodríguez, A., and Ouillo, S.: Modelling of the Ebro River plume. Validation with field observations, *Scientia Marina*, 67, 379–391, 2003.

O'Donnell, J.: The dynamics of estuary plumes and fronts, in: *Contemporary Issues in Estuarine Physics*, edited by Valle-Levinson, A., p. 186–246, Cambridge University Press, <https://doi.org/10.1017/CBO9780511676567.009>, 2010.

415 Olita, A., Ribotti, A., Sorgente, R., Fazioli, L., and Perilli, A.: SLA - chlorophyll-a variability and covariability in the Algero-Provençal Basin (1997–2007) through combined use of EOF and wavelet analysis of satellite data, *Ocean Dynamics*, 61, 89–102, <https://doi.org/10.1007/s10236-010-0344-9>, 2011a.

Osadchiev, A., Sedakov, R., and Barymova, A.: Response of a small river plume on wind forcing, *Frontiers in Marine Science*, 2021.

Penven, P., Debreu, L., Marchesiello, P., and McWilliams, J. C.: Evaluation and application of the ROMS 1-way embedding procedure to the central California upwelling system, *Ocean Modelling*, 12, 157–187, <https://doi.org/10.1016/j.ocemod.2005.05.002>, 2006.

420 Peterson, J. O. and Peterson, W. T.: Influence of the Columbia River plume (USA) on the vertical and horizontal distribution of mesozooplankton over the Washington and Oregon shelf, *ICES Journal of Marine Science*, 65, 477–483, <http://icesjms.oxfordjournals.org/>, 2008.

Piñones, A., Valle-Levinson, A., Narváez, D. A., Vargas, C. A., Navarrete, S. A., Yuras, G., and Castilla, J. C.: Wind-induced diurnal variability in river plume motion, *Estuarine, Coastal and Shelf Science*, 65, 513–525, <https://doi.org/10.1016/j.ecss.2005.06.016>, 2005.

425 Rojas, C. M., Saldías, G. S., Flores, R. P., Vásquez, S. I., Salas, C., and Vargas, C. A.: A modeling study of hydrographic and flow variability along the river-influenced coastal ocean off central Chile, *Ocean Modelling*, 181, 102 155, <https://doi.org/10.1016/j.ocemod.2022.102155>, 2023.

Salcedo-Castro, J., de Camargo, R., Marone, E., and Sepúlveda, H.: Using the mean pressure gradient and NCEP/N-CAR reanalysis to estimate the strength of the South Atlantic Anticyclone, *Dynamics of Atmospheres and Oceans*, 71, <https://doi.org/10.1016/j.dynatmoce.2015.06.003>, 2015.

430 Salcedo-Castro, J., Saldías, G., Saavedra, F., and Donoso, D.: Climatology of Maipo and Rapel river plumes off Central Chile from numerical simulations, *Regional Studies in Marine Science*, 38, <https://doi.org/10.1016/j.rsma.2020.101389>, 2020.

Saldías, G. S. and Lara, C.: Satellite-derived sea surface temperature fronts in a river-influenced coastal upwelling area off central – southern Chile, *Regional Studies in Marine Science*, 37, 101 322, <https://doi.org/10.1016/j.rsma.2020.101322>, 2020.

435 Saldías, G. S., Sobarzo, M., Largier, J., Moffat, C., and Letelier, R.: Seasonal variability of turbid river plumes off central Chile based on high-resolution MODIS imagery, *Remote Sensing of Environment*, 123, 220–233, <https://doi.org/10.1016/j.rse.2012.03.010>, 2012.

Saldías, G. S., Kipp Shearman, R., Barth, J. A., and Tufillaro, N.: Optics of the offshore Columbia River plume from glider observations and satellite imagery, *Journal of Geophysical Research: Oceans*, 121, 2367–2384, 2016.

Saldías, G. S., Largier, J. L., Mendes, R., Pérez-Santos, I., Vargas, C. A., and Sobarzo, M.: Satellite-measured interannual variability of turbid river plumes off central-southern Chile: Spatial patterns and the influence of climate variability, *Progress in Oceanography*, 146, 212–222, 440 <https://doi.org/10.1016/j.pocean.2016.07.007>, 2016.

Shchepetkin, A. F. and McWilliams, J. C.: The regional oceanic modeling system (ROMS): A split-explicit, free-surface, topography-following-coordinate oceanic model, *Ocean Modelling*, 9, 347–404, <https://doi.org/10.1016/j.ocemod.2004.08.002>, 2005.

Simpson, J.: The shelf-sea fronts: implications of their existence and behaviour, *Philosophical Transactions of the Royal Society of London*, 445 *Series A, Mathematical and Physical Sciences*, 302, 531–546, 1981.

Simpson, J. H., Allen, C. M., and Morris, N. C. G.: Fronts on the continental shelf, *Journal of Geophysical Research: Oceans*, 83, 4607–4614, <https://doi.org/https://doi.org/10.1029/JC083iC09p04607>, 1978.

Strub, P. T., Mesías, J. M., Montecino, V., Rutlant, J., and Salinas, S.: Coastal ocean circulation off western South America, in: *The Sea*, Volume 11, edited by Robinson, A. R. and Brink, K. H., pp. 273–313, John Wiley and Sons Inc, 1998.

Torrence, C. and Compo, G. P.: A practical guide to wavelet analysis, *Bull. Am. Meteor. Soc.*, 79, 61–78, 450 1998.

Vargas, C. A., Narva, D. A., Piñones, A., Navarrete, S. A., and Lagos, N. A.: River plume dynamic influences transport of barnacle larvae in the inner shelf off central Chile, *Journal of the Marine Biological Association of the United Kingdom*, 86, 1057–1065, 2006.

Warrick, J. A., A.k. Mertes, L., Washburn, L., and A. Siegel, D.: A conceptual model for river water and sediment dispersal in the Santa Barbara Channel, California, *Continental Shelf Research*, 24, 2029–2043, <https://doi.org/10.1016/j.csr.2004.07.010>, 2004.

Winckler, P., Aguirre, C., Farías, L., Contreras-López, M., and Masotti, Í.: Evidence of climate-driven changes on atmospheric, hydrological, and oceanographic variables along the Chilean coastal zone, *Climatic Change*, 163, 633–652, <https://doi.org/10.1007/s10584-020-02805-3>, 2020.

Yu, L.: Sea-surface salinity fronts and associated salinity-minimum zones in the tropical ocean, *Journal of Geophysical Research: Oceans*, 120, 4205–4225, <https://doi.org/10.1002/2015JC010790>. Received, 2015.

Zhi, H., Wu, H., Wu, J., Zhang, W., and Wang, Y.: River Plume Rooted on the Sea-Floor: Seasonal and Spring-Neap Variability of the Pearl River Plume Front, *Frontiers in Marine Science*, 9, 1–17, <https://doi.org/10.3389/fmars.2022.791948>, 2022.